J|A|C|S
ARTICLES
Published on Web 07/13/2002

Electron and Mass Transport in Hybrid Redox Polyether Melts Contacted with Carbon Dioxide

Dongil Lee, John C. Hutchison, Anthony M. Leone, Joseph M. DeSimone,* and Royce W. Murray*

Contribution from the Kenan Laboratories of Chemistry and NSF Science & Technology Center for Environmentally Responsible Solvents and Processes, University of North Carolina, Chapel Hill, North Carolina 27599

Received March 15, 2002

Abstract: Films of neat metal salts with covalently attached oligoether side chains ([Co(bpy(CO_2MePEG-350)$_2$)$_3$](ClO_4)$_2$; bpy is 2,2′-bipyridine, and MePEG-350 is methyl-terminated oligomeric ethylene oxide with an average molecular weight of 350 Da) undergo marked changes in physical and electrochemical properties upon contact with CO_2. Electrochemical measurements indicate that the physical diffusion coefficient (D_{PHYS}) of the Co(II) species, the observed rate constant for Co(II/I) self-exchange (k_{EX}), and the physical diffusion coefficient of the perchlorate counterion (D_{ClO4}) increase from 2.4×10^{-11} to 7.0×10^{-10} cm^2/s, 6.8×10^5 to 4.5×10^6 M^{-1} s^{-1}, and 3.4×10^{-10} to 4.3×10^{-9} cm^2/s, respectively, as CO_2 pressure is increased from 0 to 2000 psi at 23 °C. A reduction in activation energy accompanies the enhancement of each of these properties over this pressure range. Increasing CO_2 pressure from ambient to 1000 psi causes the films to swell 13%, and free-volume theory explains the enhanced mass transport properties of the films. The origin of increases in electron-transfer kinetics is considered. Plots of log(k_{EX}) versus log(D_{PHYS}) and log(k_{EX}) versus log(D_{ClO4}) are both linear. This suggests that electron self-exchange is controlled by factors that also affect log(D_{PHYS}) or log(D_{ClO4}). One explanation is based on plasticization of the oligoether side-chain motions by CO_2 that affect ether dipole repolarization and Co complex diffusion rates. A second explanation for the changes in k_{EX} is based on control of electron transfer by relaxation of counterions neighbor to the Co complexes, which is measured by D_{ClO4}. Both explanations represent a kind of solvent dynamics control of k_{EX}.

Introduction

Over the past decade, the use of liquid and supercritical CO_2 ($scCO_2$) to selectively control and manipulate the physical properties of polymer melts during synthesis[1] and processing[2] has become a fundamentally and technologically important subject. The ability to tune the physical properties of CO_2 by changing pressure and temperature allows for the manipulation of the physical properties of a polymer via CO_2-sorption. While CO_2-induced plasticization and depression of glass transition temperature (T_g) have been studied extensively in many systems,[3] experimental evidence that delineates the molecular factors controlling *transport* dynamics in CO_2-swollen polymer is still limited.

The adaptation of voltammetric methods to CO_2-based media is challenging owing to the low dielectric strength. The low solubility of polar solutes and tight ion pairing in CO_2 makes quantitative voltammetry difficult, even with microelectrodes. We showed some time ago, however, that a thin ionically conductive film contacting all of the electrodes of the cell made quantitative voltammetry possible even if the surrounding medium were completely ion free (e.g., a vacuum or inert gas).[4] Michael and Wightman used this same approach in obtaining well-defined voltammetry of ferrocene in CO_2, using conductive films based on Nafion[5] and PEO-based polymers.[6]

* To whom correspondence should be addressed. E-mail: rwm@email.unc.edu.

(1) (a) Kendall, J. L.; Canelas, D. A.; Young, J. L.; DeSimone, J. M. *Chem. Rev.* **1999**, *99*, 543. (b) Burke, A. L. C.; Maier, G.; DeSimone, J. M. *Polym. Mater. Sci. Eng.* **1996**, *74*, 248. (c) Gross, S. M.; Roberts, G. W.; Kiserow, D. J.; DeSimone, J. M. *Macromolecules* **2000**, *33*, 40. (d) Givens, R. D.; Jikei, M.; DeSimone, J. M. *Polym. Prepr. (Am. Chem. Soc., Div. Polym. Chem.)* **1997**, *38*, 468. (e) DeSimone, J. M.; Maury, E. E.; Menceloglu, Y. Z.; McClain, J. B.; Romack, T. J.; Combes, J. R. *Science* **1994**, *265*, 356.

(2) (a) Kazarian, S. G. *Polym. Sci. Ser. C* **2000**, *42*, 78. (b) Royer, J. R.; Gay, Y. J.; Desimone, J. M.; Khan, S. A. *J. Polym. Sci., Part B: Polym. Phys.* **2000**, *38*, 3168. (c) Cooper, A. I. *J. Mater. Chem.* **2000**, *10*, 207. (d) Kirby, C. F.; McHugh, M. A. *Chem. Rev.* **1999**, *99*, 565. (e) Marr, R.; Gamse, T. *Chem. Eng. Process.* **2000**, *39*, 19.

(3) (a) Wissinger, R. G.; Paulaitis, M. E. *J. Polym. Sci., Part B: Polym. Phys.* **1987**, *25*, 2497. (b) Garg, A.; Gulari, E.; Manke, C. W. *Macromolecules* **1994**, *27*, 5643. (c) Goel, S. K.; Beckman, E. J. *Polymer* **1993**, *34*, 1410. (d) Condo, P. D.; Paul, D. R.; Johnston, K. P. *Macromolecules* **1994**, *27*, 365. (e) Chiou, J. S.; Barlow, J. W.; Paul, D. R. *J. Appl. Polym. Sci.* **1985**, *30*, 2633. (f) Shieh, Y.-T.; Su, J.-H.; Manivannan, G.; Lee, P. H. C.; Sawan, S. P.; Spall, W. D. *J. Appl. Polym. Sci.* **1996**, *59*, 707.

(4) (a) Pickup, P. G.; Kutner, W.; Leidner, C. R.; Murray, R. W. *J. Am. Chem. Soc.* **1984**, *106*, 1991. (b) Jernigan, J. C.; Chidsey, C. E. D.; Murray, R. W. *J. Am. Chem. Soc.* **1985**, *107*, 2824. (c) Reed, R. A.; Geng, L.; Murray, R. W. *J. Electroanal. Chem. Interfacial Electrochem.* **1986**, *208*, 185. (d) Geng, L.; Reed, R. A.; Kim, M. H.; Wooster, T. T.; Oliver, B. N.; Egekeze, J.; Kennedy, R. T.; Jorgenson, J. W.; Parcher, J. F.; Murray, R. W. *J. Am. Chem. Soc.* **1989**, *111*, 1614.

(5) (a) Michael, A. C.; Wightman, R. M. *Anal. Chem.* **1989**, *61*, 270. (b) Michael, A. C.; Wightman, R. M. *Anal. Chem.* **1989**, *61*, 2193. (c) Sullenberger, E. F.; Michael, A. C. *Anal. Chem.* **1993**, *65*, 3417.

(6) (a) Sullenberger, E. F.; Michael, A. C. *Anal. Chem.* **1993**, *65*, 2304. (b) Dressman, S. F.; Michael, A. C. *Anal. Chem.* **1995**, *67*, 1339.

10.1021/ja026209p CCC: $22.00

Our previous work[7] has demonstrated that combining redox-active moieties with polyether oligomers produces amorphous, viscous, room-temperature melts. These hybrid redox-active polyethers are good model media in which to study mass and charge transport in semisolid systems. The polyether chains serve as a semirigid "solvent" shell whose properties influence the dynamics of mass and charge transport. Dissolution of other small molecules in the hybrid redox polyethers generally accelerates transport properties; this has been referred to[8] as plasticization.

This paper describes the Co(III/II) and Co(II/I) voltammetry of thin films of a polyether-tailed cobalt complex melt that are contacted by a CO_2 phase and which coat an electrochemical cell composed of working micro-, reference, and counter electrodes exposed on a miniature platform.[7] The metal complex is $[Co(bpy(CO_2MePEG\text{-}350)_2)_3](ClO_4)_2$, the ligand for which is shown below. The polyether "tail", MePEG-350, is methyl-terminated with an average of 7.2 ethylene oxide repeat units.

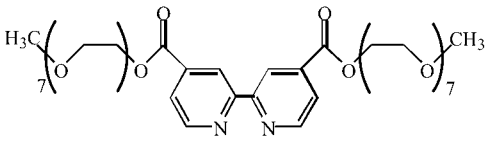

$bpy(CO_2MePEG\text{-}350)_2$

CO_2 permeates into and swells the metal complex melt film to a degree dependent on the CO_2 pressure, but without changing the chemical identity of the redox-active Co complex. The degree of CO_2 swelling and the resultant plasticization strongly influence the rates both of physical diffusion of the Co(II) complex in the melt and of electron transfers between Co(II) and Co(I) states of the complex. The ionic conductivity of the melt is also enhanced upon swelling with CO_2, which has been seen before for PEO-based films.[6] The results serve to quantify the degree of CO_2-plasticization, a measurement of practical importance for polymer synthesis and processing in CO_2 media.

The transport results further reveal a near-linear correlation between plasticization-induced changes in the rate of physical diffusion of the Co(II) complex in the melt and of the rate of Co(II/I) electron transfers. We interpret the observed correlation, as have been other diffusion rate−electron-transfer rate proportionality observations,[9] as evidence for so-called solvent dynamics control of the electron-transfer rate. We also know that homogeneous electron-transfer rates in semisolid redox-active polyether melts are generally slower and exhibit larger thermal activation barriers[7,10] than those for analogous reactions in dilute fluid solutions, and are larger than (outer-sphere) reorganization energy barriers predicted from classical Marcus theory.[11] The reason(s) for these differences are an ongoing part of our investigations. The contribution of the thermal barrier associated with repolarization of the ether (or other) dipoles in the "solvent shell" (i.e., solvent dynamics activation energy) has been suggested[10] as one possibility. Another possibility, briefly explored here, is the dynamics of relaxation of the counterions surrounding reacting electron donor−acceptor pairs.

Experimental Section

Reagents. SFC/SFE grade of CO_2 (Air Products) was used as received. The polyether-tailed bipyridine ligand $bpy(CO_2MePEG\text{-}350)_2$ and its cobalt complex melt were synthesized as described previously.[10a]

High-Pressure Microelectrode Cell Fabrication. The microelectrode cell onto which a film of the Co complex melt was cast and used for voltammetry under high pressure consists of the tips of four wires exposed in an insulating plane: a small-diameter (25 μm diameter, Goodfellow) Pt wire working electrode, two Pt (0.4 mm diameter) wire electrodes, and a Ag (0.5 mm diameter) wire quasi-reference electrode. Three-electrode voltammetry made use of one of the two 0.4 mm Pt wires as counter electrode. The two 0.4 mm Pt wire electrodes were used in measuring the ionic conductivities of the melts. The wires were connected to 22-gauge magnet wire (Belden) with silver epoxy (Epo-Tek H2OE, Epoxy Technology Inc.); they were protected from shorting to one another by the insulating coating of the magnet wire. The group of four electrodes was inserted through a $^1/_4$ in. stainless steel tube and potted in place with an epoxy resin (poly(bisphenol A-*co*-epichlorohydrin), glycidyl end-capped, M_n ca. 377; Aldrich) cross-linked with 14 wt % 1,3-phenylenediamine (Aldrich). (In early trials, the working electrode was sealed in a glass capillary, which exhibited poor pressure durability, and the microwire was (carefully) potted in place with the others in a naked form.) The end of the assembly was polished with alumina paste (successively smaller grades down to 0.05 μm; Buehler) and cleaned electrochemically in 0.1 M H_2SO_4 solution,[12] to make a cell platform onto which the Co complex melt was cast.

High-Pressure Electrochemical Cell. The high-pressure cylindrical view cell was constructed of 316 stainless steel with a cavity volume of 25 mL. Two sapphire windows (1 in. diameter and $^3/_8$ in. thickness, Crystal Systems) were mounted into opposing sides of the cell bottom and held in place with hollow brass bolts and Teflon O-rings. Three $^1/_{16}$ in. Taper Seal ports (High-Pressure Equipment's standard) were machined in the cell for CO_2 inlet/outlet and thermocouple connections. One $^1/_4$ in. NPT port was tapped into the cell for the microelectrode probe. Temperature control of the cell was maintained within $\pm$0.5 °C of the set temperature using a water jacket connected to temperature controller (Model RTE-110, Neslab). The pressure within the cell was monitored using an output pressure transducer (Model TJE AP121DV, Sensotec). High-pressure CO_2 was introduced to the cell using a syringe pump (Model 260D, Isco). As a precaution, a safety head equipped with a 7000 psi rupture disk (High-Pressure Equipment) is included in the plumbing between the pump and the cell.[13]

High-Pressure Swelling Cell. To measure CO_2 swelling of the Co complex melt, we employed our previously described high-pressure cell specifically designed to measure volumes at elevated CO_2 pres-

(7) (a) Velazquez, C. S.; Hutchison, J. E.; Murray, R. W. *J. Am. Chem. Soc.* **1993**, *115*, 7896. (b) Poupart, M. W.; Velazquez, C. S.; Hassett, K.; Porat, Z.; Haas, O.; Terrill, R. H.; Murray, R. W. *J. Am. Chem. Soc.* **1994**, *116*, 1165. (c) Long, J. W.; Kim, I. K.; Murray, R. W. *J. Am. Chem. Soc.* **1997**, *119*, 11510. (d) Pyati, R.; Murray, R. W. *J. Am. Chem. Soc.* **1996**, *118*, 1743. (e) Dickinson, E. V.; Williams, M. E.; Hendrickson, S. M.; Masui, H.; Murray, R. W. *J. Am. Chem. Soc.* **1999**, *121*, 613.

(8) (a) Geng, L.; Longmire, M. L.; Reed, R. A.; Parcher, J. F.; Barbour, C. J.; Murray, R. W. *Chem. Mater.* **1989**, *1*, 58. (b) Barbour, C. J.; Murray, R. W.; Parcher, J. F. *Anal. Chem.* **1991**, *63*, 604.

(9) (a) Zhang, X.; Leddy, J.; Bard, A. J. *J. Am. Chem. Soc.* **1985**, *107*, 3719. (b) Zhang, X.; Yang, H.; Bard, A. J. *J. Am. Chem. Soc.* **1987**, *109*, 1916. (c) Miao, W.; Ding, Z.; Bard, A. J. *J. Phys. Chem. B* **2002**, *106*, 1392. (d) Gu, N.; Zhou, H.; Ding, L.; Shi, Z.; Dong, S. *Solid State Ionics* **2000**, *138*, 123. (e) Zhou, H.; Dong, S. *J. Electroanal. Chem.* **1997**, *425*, 55.

(10) (a) Williams, M. E.; Masui, H.; Long, J. W.; Malik, J.; Murray, R. W. *J. Am. Chem. Soc.* **1997**, *119*, 1997. (b) Williams, M. E.; Lyons, L. J.; Long, J. W.; Murray, R. W. *J. Phys. Chem. B* **1997**, *101*, 7584. (c) Dickinson, E. V.; Masui, H.; Williams, M. E.; Murray, R. W. *J. Phys. Chem. B* **1999**, *103*, 11028.

(11) (a) Marcus, R. A.; Sutin, N. *Biochim. Biophys. Acta* **1985**, *811*, 265. (b) Marcus, R. A.; Siddarth, P. In *Photoprocesses in Transition Metal Complexes, Biosystems, and Other Molecules*; Kochanski, E., Ed.; Kluwer Academic Publishers: Dordrecht, The Netherlands, 1992. (c) Sutin, N. *Acc. Chem. Res.* **1982**, *15*, 275. (d) Sutin, N. *Prog. Inorg. Chem.* **1983**, *30*, 441.

(12) Conway, B. E.; Angerstein-Kozlowska, H.; Sharp, W. B. A.; Criddle, E. E. *Anal. Chem.* **1973**, *45*, 1331.

(13) For safety information regarding handling of high-pressure apparatus, see, for example, ref 6a.

sure.[14] Briefly, the rectangular cell is 6.35 mm wide, 15.87 mm deep, and 15.87 mm high, and is designed to constrain swelling of the polymer sample to one dimension so that the volume change can be easily quantified with optical images captured by a digital camera. An image capture board (Scion Corp LG3) and NIH imaging software were used to correlate the number of pixels occupied by the polymer volume in the image with the calibration of the pixels. Because of the large sample size employed here (~0.5 mL), a long equilibration time (12−24 h) was allowed prior to the measurements.

Electrochemical Measurements. Cyclic voltammetry and chronoamperometry of the Co complex melt film were performed at different CO_2 pressures using a home-built low-current potentiostat and locally written data acquisition software. Films of the Co complex melts (ca. 1 mm thick), which are infinitely thick relative to the voltammetric diffusion layers, were cast onto the microelectrode platform and thoroughly dried under vacuum (ca. 1×10^{-3} Torr) in the high-pressure cell at 70 °C for 3 days. Films were equilibrated at each temperature and pressure for at least 2 h prior to measurements. The peak potentials of the Co(II/I) and Co(III/II) waves were determined by cyclic voltammetry. Apparent diffusion coefficients (D_{APP}) for the Co(II/I) and Co(III/II) reactions were determined by chronoamperometry using 400−500 mV potential steps from a non-Faradaic region to diffusion-limited potentials of the waves. Current−time responses were typically analyzed for times up to 30 s. Owing to the slow transport rates in the semisolid melts, the diffusion geometry is linear on this short time scale.[15] The current decay for the linear region was accordingly analyzed with the Cottrell equation:

$$I = nFAD^{1/2}C/\pi^{1/2}t^{1/2} \quad (1)$$

where I is the current, F is Faraday's constant, A is the microelectrode area, D is the diffusion coefficient, C is the concentration (mol/cm^3), and t is the time. The radius of the microelectrode (14 μm) was calibrated by voltammetry of ferrocene.[16]

Ionic conductivities of the melts were measured using a Solartron Model SI 1260 impedance/gain phase analyzer−SI 1287 electrochemical interface combination over a frequency range from 1 MHz to 1 Hz. The dc bias was held at −0.2 V, while the ac amplitude was set to 50 mV. Conductivity was calculated as the product of geometric cell constant (7.5 cm^{-1}) and cell resistance (taken from the low-frequency real-axis intercept of the complex impedance semicircle).

Results and Discussion

CO_2-Induced Swelling Volume Measurements. In the electrochemical measurements, the Co complex melt films were exposed to CO_2 at pressures up to 2000 psi. To account for the concentration change of the Co complexes in the melt upon swelling by imbibed CO_2, optical swelling volume measurements were performed at constant temperature and varied CO_2 pressure. The swelling behavior of the Co complex melt as a function of CO_2 pressure (Figure 1) shows that the volume increases modestly (13%) with increasing CO_2 pressure up to 1000 psi and then levels off. Measurements carried out at combinations of temperature (from 23 to 50 °C) and pressure (up to 800 psi) corresponding to constant CO_2 density show essentially no volume change. From these results, we conclude that CO_2 partitioning into and swelling of the Co complex melt is temperature invariant in the temperature range covered in the activation barrier energy measurements (vide infra).

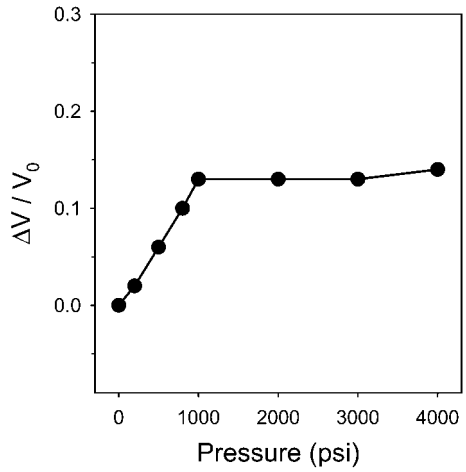

Figure 1. CO_2 pressure dependence of the swelling volume (ΔV) at 23 °C relative to the initial volume (V_0) of $[Co(bpy(CO_2MePEG\text{-}350)_2)_3](ClO_4)_2$ melt under vacuum.

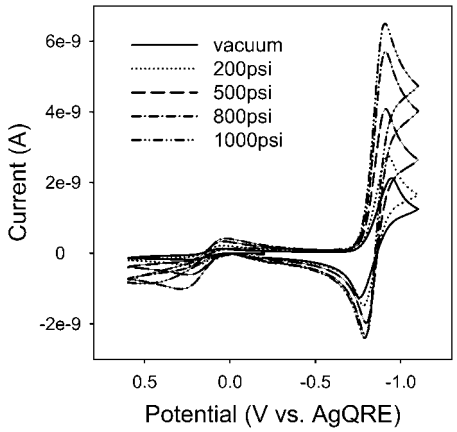

Figure 2. Cyclic voltammograms (5 mV/s) of $[Co(bpy(CO_2MePEG\text{-}350)_2)_3](ClO_4)_2$ melt at 14 μm radius Pt microdisk electrode at 23 °C and at indicated CO_2 pressures.

Voltammetry and Transport Measurements in Co Complex Melt Contacted with CO_2. Figure 2 shows voltammograms of the polyether-tailed Co complex melt, $[Co(bpy(CO_2MePEG\text{-}350)_2)_3](ClO_4)_2$, at various CO_2 pressures. Like previously reported work on Co complex polyether hybrids,[10] the Co(II/I) reduction currents at −0.85 V greatly exceed those for Co(III/II) oxidation at 0.15 V at all pressures. The difference in currents arises from the facile electron self-exchange reactions (hopping) in the Co(II/I) mixed-valent diffusion layer in the electrode/melt interfacial region. Electron hopping is unimportant in the Co(III/II) diffusion layer owing to the negligibly small electron self-exchange rate constant (k_{EX}) for the low-spin Co(III)/high-spin Co(II) reaction.[17] The diffusion coefficient of the Co(III/II) couple thus measures the physical diffusion coefficient (D_{PHYS}) of the Co(II) complex, while that of the Co(II/I) couple is an apparent diffusion coefficient (D_{APP}) consisting of the summation of physical and electron (hopping) diffusion according to the Dahms−Ruff equation:[18]

$$D_{APP} = D_{PHYS} + D_E = D_{PHYS} + \frac{k_{EX}\delta^2 C}{6} \quad (2)$$

(14) Royer, J. R.; DeSimone, J. M.; Khan, S. A. *Macromolecules* **1999**, *32*, 8965.
(15) (a) Gravity-convection effects on transport are not observed in these viscous media even at much longer time.[15b] (b) Crooker, J. C.; Murray, R. W. *Anal. Chem.* **2000**, *72*, 3245.
(16) Owlia, A.; Wang, Z.; Rusling, J. F. *J. Am. Chem. Soc.* **1989**, *111*, 5091.
(17) Buttry, D. A.; Anson, F. C. *J. Am. Chem. Soc.* **1983**, *105*, 685.

Table 1. Physical Dynamics and Electron-Transfer Results for $[Co(bpy(CO_2MePEG\text{-}350)_2)_3](ClO_4)_2$ Melt at a Series of CO_2 Pressures

CO_2 density (g/mL)	0.000	0.027	0.078	0.163	0.770	0.877
CO_2 pressure (psi) at 23 °C	vacuum	200	500	800	1000	2000
concentration[a] of Co (M)	0.445	0.436	0.419	0.403	0.394	0.393
δ (Å)	15.5	15.6	15.8	16.0	16.2	16.2
D_{PHYS}[b] (23 °C) Co(III/II) (cm^2/s)	2.4×10^{-11}	8.3×10^{-11}	2.4×10^{-10}	5.8×10^{-10}	6.2×10^{-10}	7.0×10^{-10}
D_{ClO4}[c] (23 °C) (cm^2/s)	3.4×10^{-10}	8.5×10^{-10}	2.1×10^{-9}	3.7×10^{-9}	4.3×10^{-9}	4.3×10^{-9}
D_E[d] (23 °C) Co(II/I) (cm^2/s)	1.2×10^{-9}	1.9×10^{-9}	3.3×10^{-9}	5.6×10^{-9}	7.3×10^{-9}	7.7×10^{-9}
$E_{A,PHYS}$[e] (kJ/mol)	60	48	35	25		
$E_{A,ION}$[e] (kJ/mol)	44	36	23	20		
$E_{A,ET}$[f] (kJ/mol)	36	33	26	21		
t_{ClO4}[g] (23 °C)	0.84	0.84	0.82	0.76	0.78	0.75
D_{ClO4}/D_E	0.29	0.45	0.64	0.65	0.60	0.54
k_{EX}[h] (23 °C) ($M^{-1}\,s^{-1}$)	6.8×10^5	1.1×10^6	1.9×10^6	3.3×10^6	4.2×10^6	4.5×10^6
$k_{EX}{}^0$[i] (23 °C) ($M^{-1}\,s^{-1}$)	1.5×10^{12}	7.8×10^{11}	8.1×10^{10}	1.7×10^{10}		
$\exp(-\Delta G^*/RT)$[j] (23 °C)	4.4×10^{-7}	1.5×10^{-6}	2.6×10^{-5}	2.0×10^{-4}		

[a] Concentrations are estimated from swelling volume measurements. [b] From Cottrell slope (eq 1) chronoamperometry. [c] Calculated from eq 3. [d] Calculated from eq 2. [e] From slopes of activation plots in Figure 4. [f] From slopes of activation plots in Figure 6. [g] Transference number for the ClO_4^- counterion. [h] Calculated via eq 2. [i] Intercepts of activation plots of k_{EX} as in Figure 6, converted to rate constants using eq 2. [j] Calculated by using $E_{A,ET}$ values for ΔG^*.

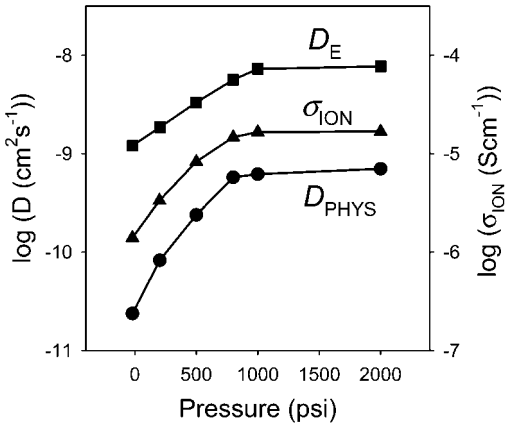

Figure 3. CO_2 pressure dependencies of D_{PHYS}, D_E, and σ_{ION} in $[Co(bpy(CO_2MePEG\text{-}350)_2)_3](ClO_4)_2$ melt at 23 °C.

where D_E is the electron diffusion coefficient, δ is the equilibrium center-to-center distance[19] between complexes, and C is the total concentration of Co complex sites in the melts. The diffusion constant values that control currents in the Co(III/II) D_{PHYS} and Co(II/I) reactions D_E ($=D_{APP} - D_{PHYS}$) were determined using chronoamperometry. The Co complex concentrations, C, were corrected for swelling associated with the CO_2-sorption (see Supporting Information Table S1). The diffusion constants obtained at 23 °C as a function of CO_2 pressure are presented in Figure 3 and Table 1. Both D_{PHYS} and D_E are remarkably dependent on CO_2 pressure, increasing by ca. 26-fold and 6-fold, respectively, at 1000 psi relative to vacuum. Electron-transfer rate constants (k_{EX}) calculated from eq 2 and given in Table 1 change with pressure by similar amounts. The values tend to plateau at the highest pressures.

Increases in solute mass transfer rate in CO_2-swollen polymer matrixes have been observed in many systems. For example, Dooley and co-workers observed an increase of 10^6-fold in the diffusivity of ethylbenzene in polystyrene contacted by $scCO_2$.[20] The enhanced diffusion of azobenzene in CO_2-swollen polystyrene, measured using forced Rayleigh scattering,[21] was discussed in terms of plasticization and subglass relaxations associated with local polymer dynamics. In a voltammetric study, Sullenberger and Michael[6a] found that the ionic conductivity of high molecular weight PEO-based films is affected by CO_2 swelling of the amorphous domain of the partially crystalline polyether phase. The polyether-tailed Co complex used here relies on low molecular weight polyether and is an amorphous melt above ambient temperature, as shown by earlier thermal measurements.[10a] Polymer diffusion-plasticization effects[8] of small molecules on polyether media have been detected by electrochemical measurements, as noted above.

Figure 3 also shows the CO_2-pressure dependency of ionic conductivity (σ_{ION}) of the Co complex melt, which increases with increasing CO_2 pressure in a manner quite similar to that of D_{PHYS}. The diffusivity of the Co(II) complex, D_{PHYS}, and that of the ClO_4^- counterion (D_{ClO4}) are related to σ_{ION} by the Nernst−Einstein relation:[10b,22]

$$\sigma_{ION} = \frac{F^2}{RT}[z_{Co}^2 D_{Co} C_{Co} + z_{ClO4}^2 D_{ClO4} C_{ClO4}] \qquad (3)$$

where z, D, and C are charge, diffusion coefficient, and concentration of the indicated species, respectively. Table 1 shows calculated values of D_{ClO4} from which we see that the ClO_4^- counterion is 5−15-fold more mobile diffusively than the Co complex. Figure 4 shows activation barrier plots for D_{PHYS} and σ_{ION}; Table 1 presents the results.[23] The activation energy barrier for D_{PHYS} is larger than that of σ_{ION}, and both energy barriers decrease with increasing CO_2 pressure. The difference between D_{PHYS} and σ_{ION} is not surprising given the difference in size of these ions and in light of the fact that the Co complex bears the polyether tails. Mass transport in polyether matrixes involves deformation and segmental motions of the polymer chains, so transport of larger ions should be both slower and more energy intensive than that of smaller ones. The differences between D_{PHYS} of the Co complex and D_{ION} of its

(18) (a) Dahms, H. *J. Phys. Chem.* **1968**, *72*, 362. (b) Ruff, I.; Friedrich, V. J. *J. Phys. Chem.* **1971**, *75*, 3297. (c) Majda, M. In *Molecular Design of Electrode Surfaces*; Murray, R. W., Ed.; John Wiley & Sons: New York, 1992; pp 159−206.

(19) δ is taken as the equilibrium center-to-center distance between Co complexes and is calculated from the melt density on the basis of a cubic lattice model.[10a] For CO_2-swollen Co complex melt, δ values are estimated from the swelling volume measurements. See Supporting Information Table S1 for details.

(20) Dooley, K. M.; Launey, D.; Becnel, J. M.; Caines, T. L. *ACS Symp. Ser.* **1995**, *608 (Innovations in Supercritical Fluids)*, 269.

(21) Chapman, B. R.; Gochanour, C. R.; Paulaitis, M. E. *Macromolecules* **1996**, *29*, 5635.

(22) MacCallum, J. R.; Vincent, C. A. *Polymer Electrolyte Reviews*; Elsevier Applied Science: Oxford, U.K., 1987; Vol. 1.

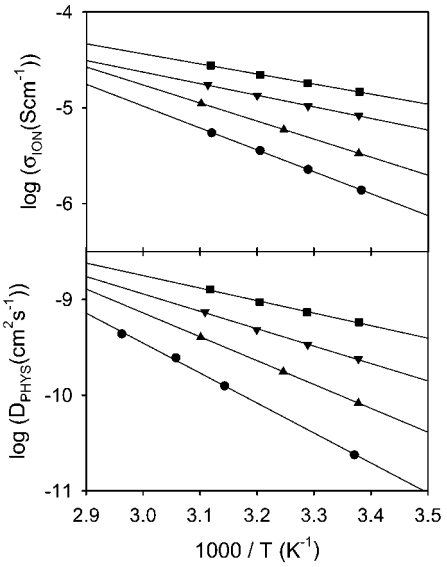

Figure 4. Activation plots of σ_{ION} (upper plots) and D_{PHYS} (lower plots) at a series of initial CO_2 pressures: vacuum (●), 200 (▲), 500 (▼), and 800 psi (■).

perchlorate counterion, and between their respective activation barriers, are largest in a vacuum and decrease with increasing CO_2 pressure, which reflects the plasticizing effect of the imbibed CO_2. We interpret the partitioned CO_2 as facilitating the required polyether chain segmental motions.

Effect of CO_2-Swelling on Mass Transport: Free Volume Theory. The remarkable similarity in pressure dependence of swelling volume and mass transport ($\log(D_{PHYS})$ and $\log(\sigma_{ION})$) in Table 1 prompts us to examine these parallel effects in terms of free volume theory.[24] The fractional free volume (*FFV*) was estimated from:

$$FFV = \frac{V_m - V_w}{V_m} \tag{4}$$

where $V_m = M/\rho$ is the molar volume of the melt, M and ρ are the molecular weight and density of the melt, respectively, and V_w is the estimated van der Waals volume, calculated using a functional group contribution method.[25] The molar volumes of CO_2-swollen melts at each pressure were estimated from swelling volume measurements as described above. According

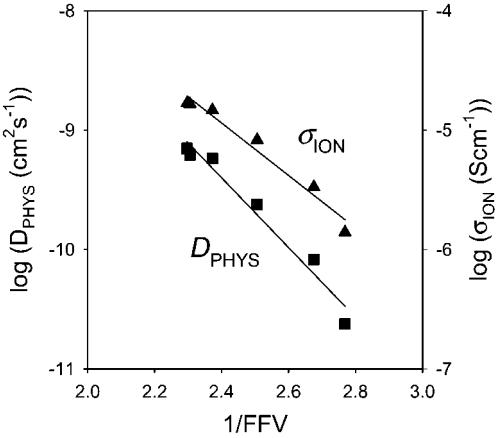

Figure 5. Relationship between physical diffusivity (D_{PHYS})/ionic conductivity (σ_{ION}) and the reciprocal fractional free volume (1/*FFV*) for CO_2-swollen $[Co(bpy(CO_2MePEG\text{-}350)_2)_3](ClO_4)_2$ melt.

to the free volume theory,[8b,24b] diffusivity should decrease exponentially with the reciprocal free volume, 1/*FFV*. Figure 5 shows that $\log(D_{PHYS})$ and $\log(\sigma_{ION})$ do vary reasonably linearly with 1/*FFV*, with negative slopes. This successful correlation of metal complex and perchlorate ion transport with free volume induced by CO_2-swelling (and, by association, with the local viscosity of the polymer matrix) implies a potential voltammetric method for determination of free volume changes in other polymeric media that exhibit a capacity for ion transport.

Effect of CO_2-Swelling on Electron-Transfer Rates. The electron diffusion coefficient D_E and corresponding rate constant k_{EX} change with CO_2 pressure in a manner similar to D_{PHYS} (Figure 3, Table 1). Increasing CO_2 pressure could affect electron transfers in the polymer in at least two ways: (a) plasticization of the polymer matrix arising from imbibed CO_2, and (b) compression from the increased hydrostatic pressure.

In regard to (b), one can expect that any significant differences between partial molar compressibilities of the oxidized and reduced species would result in a pressure dependence of the electron-transfer reaction. In fact, Swaddle et al.[26] reported that the electron-transfer kinetics of aqueous Co(III/II) *ligand* complexes vary with hydrostatic pressure over the range from ambient to ca. 30 000 psi. However, when the Co melt films are pressurized with argon over a range from ambient to 4000 psi, there was very little change in either D_{PHYS} or D_E (see Supporting Information Figure S1). We conclude that hydrostatic pressure effects are not significant and that the observed increases in electron-transfer rates are associated with CO_2-swelling and plasticization.

The temperature dependence of the electron-transfer reaction rate constant can be expressed by[11]

$$k_{EX} = K_p \kappa \nu_n \exp\left[-\frac{\Delta G^*}{RT}\right] \tag{5}$$

where, assuming a symmetrical reaction (i.e., reaction entropy of activation is zero), the activation enthalpy $E_{A,ET} \approx \Delta G^*$ ($=\lambda/$

(23) (a) Factors that might bias the transport results and activation barrier energies are electronic and ionic migration effects. Electronic migration refers to enhanced electron hopping rates driven by electric field gradients in the sample (typically arising from low ion mobility), leading to overestimation of D_E. Electronic migration becomes significant[10a,c,23b] when the ratio of counterion to electron diffusivity (D_{ClO4}/D_E) becomes much less than unity. Table 1 shows that this ratio is only slightly less than one, and, consequently, as was also shown previously[10a,b] for these melts, electronic migration effects are negligible. Calculations such as those in ref 10a,b were also carried out for the present results. The migration correction results in 10−14% lowering of D_E values, but produces essentially the same $E_{A,ET}$ values (37, 33, 26, and 21 kJ/mol at vacuum, 200, 500, and 800 psi, respectively). Ionic migration refers to mass transport aided or retarded by ionic reactants supporting part of the ion flow that accompanies electrode reactions. It is negligible when the counterion transference number (t_{ClO4})[23c,d] is unity. Table 1 shows that t_{ClO4} is only modestly less than unity, and so this effect (which would lead to underestimation of D_{PHYS}) is also not an issue. (b) Andrieux, C. P.; Saveant, J. M. *J. Phys. Chem.* **1988**, *92*, 6761. (c) $t_{ClO4} = D_{ClO4}/\Sigma(D_{Co}, D_{ClO4})$. (d) Bard, A. J.; Faulkner, L. R. *Electrochemical Methods: Fundamental and Applications*; John Wiley & Sons: New York, 1980; pp 66, 123.

(24) (a) Flory, P. J. *J. Chem. Phys.* **1950**, *18*, 108. (b) Cohen, M. H.; Turnbull, D. *J. Chem. Phys.* **1959**, *31*, 1164. (c) Stern, S. A.; Saxena, V. *J. Membr. Sci.* **1980**, *7*, 47. (d) Stern, S. A.; Frisch, H. L. *Annu. Rev. Mater. Sci.* **1981**, *11*, 523.

(25) (a) Van Krevelen, D. W.; Hoftyzer, P. J. *Properties of Polymers*; Elsevier Scientific Publishing Company: Amsterdam, 1976. (b) Van Krevelen, D. W.; Hoftyzer, P. J. *J. Appl. Polym. Sci.* **1969**, *13*, 871. (c) Bondi, A. *J. Phys. Chem.* **1964**, *68*, 441.

(26) (a) Fu, Y.; Cole, A. S.; Swaddle, T. W. *J. Am. Chem. Soc.* **1999**, *121*, 10410. (b) Swaddle, T. W. *Can. J. Chem.* **1996**, *74*, 631. (c) Grace, M. R.; Swaddle, T. W. *Inorg. Chem.* **1993**, *32*, 5597. (d) Swaddle, T. W. *Inorg. Chem.* **1990**, *29*, 5017.

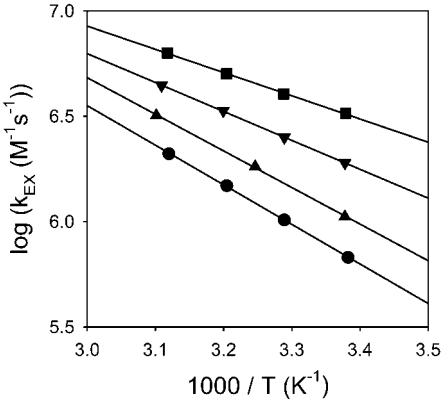

Figure 6. Activation plots of k_{EX} for Co(II/I) reaction at a series of initial CO_2 pressures: vacuum (●), 200 (▲), 500 (▼), and 800 psi (■).

4, where λ is the reorganization barrier energy), K_P is the donor−acceptor precursor complex formation constant, κ is the electronic transmission coefficient, and ν_n is the nuclear frequency factor. Figure 6 gives activation plots[27] for k_{EX}, and Table 1 gives the associated activation barrier energies, $E_{A,ET}$, and intercepts, k_{EX}^0. The results show that the activation energy $E_{A,ET}$ for homogeneous electron transfer decreases markedly as CO_2 pressure increases. The same effect was observed above for activation barriers for D_{PHYS} and σ_{ION}.

In the context of eq 5, CO_2-swelling-induced changes in the rate constant k_{EX} can arise from changes either in the activation energy barrier or in the preexponential term. On the basis of the substantial decrease in $E_{A,ET}$ with increasing CO_2 pressure seen in Table 1, one might expect k_{EX} to increase by as much as ca. 440-fold at 800 psi relative to its value in a vacuum. However, the actual increase in rate constant is only 5-fold. It is clear that factors contained in the preexponential term ($k_{EX}^0 = K_P\kappa\nu_n$) must also vary. While there is perhaps a 10-fold uncertainty in k_{EX}^0 owing to the long extrapolation from a relatively small temperature interval, Table 1 displays an obvious decrease in k_{EX}^0 with increasing CO_2 pressure. The precursor formation constant K_P is near unity[10a] and is unlikely to exhibit a large pressure dependency, so the changes in k_{EX}^0 are associated with $\kappa\nu_n$ of eq 5. The preexponential term change suggests that the electron-transfer reaction becomes less adiabatic with increasing CO_2 pressure. It is possible that the CO_2-swelling tends to weaken the electronic coupling between reactant sites. Overall, however, the electron-transfer rate constant increases with CO_2-swelling because the effect of the change in activation barrier energy exceeds that of the preexponential term.

A Correlation between Diffusion and Electron-Transfer Rates. Figure 7 displays constant-pressure log−log plots of the temperature dependencies of the electron-transfer rate constant k_{EX} and D_{PHYS}. These plots are linear with slopes ranging from 0.68 to 0.84; the higher slope corresponds to larger CO_2 pressures. The Figure 7 insets are an alternative inspection of the k_{EX} and D_{PHYS} correlation, plotting in this case isothermal data at 23 and 48 °C, the rate variations now being caused by

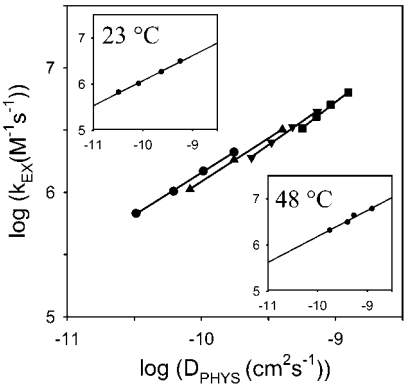

Figure 7. Relationship between k_{EX} for Co(II/I) reaction and D_{PHYS} for Co(III/II) reaction measured at various temperatures (23−48 °C) in [Co(bpy(CO_2MePEG-350)$_2$)$_3$](ClO_4)$_2$ melt at a series of CO_2 pressures: vacuum (●), 200 (▲), 500 (▼), and 800 psi (■). Slopes are 0.68, 0.70, 0.75, and 0.84 at vacuum, 200, 500, 800 psi, respectively. Insets: k_{EX} versus D_{PHYS} at 23 and 48 °C.

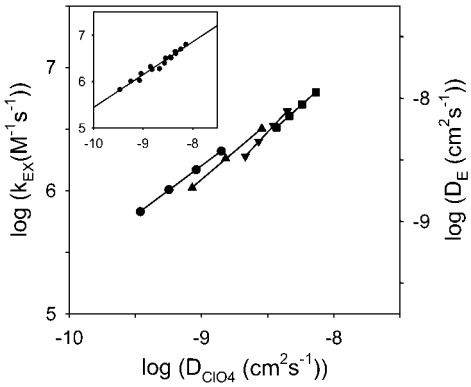

Figure 8. Relationship between k_{EX} for Co(II/I) reaction and D_{ClO4} measured at various temperatures (23−48 °C) in [Co(bpy(CO_2MePEG-350)$_2$)$_3$](ClO_4)$_2$ melt at a series of CO_2 pressures: vacuum (●), 200 (▲), 500 (▼), and 800 psi (■). Slopes are 0.80, 0.91, 1.15, and 0.96 at vacuum, 200, 500, 800 psi, respectively. Inset: k_{EX} versus D_{ClO4} at various temperatures (23−48 °C) and pressures (vacuum to 800 psi). Slope = 0.7.

changes in pressure. These plots are essentially identical at all temperatures, with a slope of 0.56. Figure 8 displays a log−log comparison between k_{EX} and D_{ClO4}, in which again a reasonably linear correlation is seen, and, in this case, the slopes are near unity ranging from 0.80 to 1.15.

For electron-exchange reactions with weak donor−acceptor electronic coupling, a dielectric continuum treatment predicts that the frequency factor is[28]

$$\nu_n = \tau_L^{-1}\left[\frac{\Delta G_{OS}^*}{4\pi RT}\right]^{1/2} \qquad (6)$$

where ΔG_{OS}^* is the outer-sphere reorganizational barrier energy, and τ_L is the longitudinal solvent relaxation time or time constant for solvent dipole repolarization. Response of electron-transfer (and other types of reaction) rates to solvent dipole repolarization time constants in this manner is termed "solvent dynamics rate" control, and this phenomenon has been widely studied. In other words, solvent properties can influence the rate constant dynamically through ν_n by reducing the barrier

(27) All temperature-dependence studies of D_E, together with D_{PHYS} and σ_{ION}, reported here were conducted at a constant CO_2 density and a variable pressure. $E_{A,ET}$ values obtained from the activation plots at constant pressure (i.e., CO_2 density is lowered to maintain constant pressure with increasing temperature) are 34, 25, 18 kJ/mol at a constant pressure of 200, 500, and 800 psi, respectively, similar to those obtained from the activation plots at a constant CO_2 density.

(28) (a) Weaver, M. J. *Chem. Rev.* **1992**, *92*, 463. (b) Fawcett, W. R.; Opallo, M. *Angew. Chem., Int. Ed. Engl.* **1994**, *33*, 2131. (c) Zusman, L. D. *Chem. Phys.* **1980**, *49*, 295. (d) Calef, D. F.; Wolynes, P. G. *J. Phys. Chem.* **1983**, *87*, 3387.

crossing frequency, provided the solvent and the transition-state motion are closely coupled.

Ordinarily, correlations between rate and τ_L are sought using dilute solutions in solvents for which τ_L is experimentally known. No such information is available for the hybrid redox polyether semisolids, and we resort to an indirect approach. It is possible to derive a relationship between τ_L, viscosity (η), and diffusion coefficients (D), which is:[28a,b,29−31]

$$\tau_L^{-1} = \left(\frac{\epsilon_S}{\epsilon_{OP}}\right)\frac{k_B T}{4\pi\eta\alpha^3} = \left(\frac{\epsilon_S}{\epsilon_{OP}}\right)\frac{3r_H D}{2\alpha^3} \quad (7)$$

where ϵ_{op} and ϵ_s are the optical and static dielectric constants, respectively, k_B is Boltzmann's constant, η is viscosity, α is molecular radius, and r_H is hydrodynamic radius. Equation 7 presents a basis for expecting a correlation between diffusivity and electron-transfer rate, such as seen in Figures 7 and 8. It should be noted, however, that the correlation is not exactly linear (i.e., the slope is not always unity). Previous solvent dynamics studies[28b,32] have also found kinetics with $\tau_L^{-\theta}$, where θ is between 0 and 1, when the reaction adiabaticity is weak or the inner-sphere reorganizational barrier is large (i.e., the dependence of the preexponential factor on solvent is weakened). Thus, we interpret the results of Figures 7 and 8 as reflecting some kind of solvent dynamics control of the Co(II/I) electron-transfer rate constant in the $[Co(bpy(CO_2MePEG\text{-}350)_2)_3](ClO_4)_2$ hybrid redox polyether melt.

There have been a number of previous observations of electron transfer−diffusivity correlations that have also been interpreted as evidence for solvent dynamic control. Bard and co-workers[9a−c] have shown that the heterogeneous rate constant (k_{HET}^0) varies with the diffusion coefficient of the reactant (and the reciprocal viscosity of the solution, $1/\eta$) in aqueous solutions. The dependence of k_{HET}^0 on the solvent has been also observed in polymer solutions.[9d−e] This laboratory has, in fact, described an ca. 11-order of magnitude range linear relation between the Co(III/II) heterogeneous rate constant (k_{HET}^0) of $Co(bpy)_3^{2+}$ complexes and D_{PHYS}, in various solvents ranging from fluids to semisolid hybrid redox polyethers.[30] This result was cited as a remarkably broad example of solvent dynamics control of the heterogeneous electron-transfer rate constant.

Because the hybrid redox polyether melts are concentrated, complex materials, and no explicit τ_L information is available for them, the specific chemical nature of the specific dipolar repolarizations that give rise to the k_{EX}/diffusion coefficient solvent dynamics correlation is unknown. We have speculated before[10] that the "solvent" dipoles are those of the polyether chains and that the τ_L is associated with the segmental motions of those chains. Physical diffusion of the metal complexes through their melts is coupled to large amplitude segmental motion of the polymer. This mutual dependency on polyether chain motions is a plausible rationale for the observed Figure 7 (Table 1) correlation between D_{PHYS} and k_{EX} values. Plasticization enhances the mobility of the polyether chains and, correspondingly, the rates of both electron transfer and physical diffusion. It is probably significant in this regard that at high plasticization, the activation barrier energies for physical diffusion and electron transfer have become rather similar and that the slope of the D_{PHYS} and k_{EX} correlation in Figure 7 is nearest unity as ideally expected from eq 7.

The ether dipoles are, however, not the sole possible source of a repolarization process. Counterion relaxation may additionally or alternatively be important. A Co(II) complex melt with 0.4 M Co sites also contains 0.8 M counterions, ClO_4^- in the present case. When a Co(II/I) electron transfer occurs, the relocation of the cationic charge will be accompanied by a redistribution of the ClO_4^- counterions. This can be portrayed in simple terms by a reversible electron-transfer step with forward and reverse rate constants k_1 and k_{-1} ($K_{EQ} = k_1/k_{-1}$), followed by a relaxation of the X^- counterion (i.e., ClO_4^-) position with rate constant k_2

$$X^-Co^{II}Co^I \underset{k_{-1}}{\overset{k_1}{\rightleftarrows}} X^-Co^ICo^{II} \xrightarrow{k_2} Co^ICo^{II}X^- \quad (8)$$

This set of reaction steps is analogous to the "electron transfer first" case discussed recently[33] by Marcus in the context of ion pairing effects on electron transfers. Note that ion pairing is intrinsic to the metal complex melts in the sense that there is no diluting solvent. The electron-transfer rate constant could be written as,

$$\frac{1}{k_{EX}} = \frac{1}{k_1} + \frac{k_{-1}}{k_2 k_1} \quad (9)$$

and the counterion relocation rate constant (k_2), as a diffusion process (D), can be modeled[33] as,

$$k_2 = D\left(\frac{\pi}{2a}\right)^2 \quad (10)$$

where a is the diffusion length of the counterion.

Inspection of these equations shows that a proportional relation between the experimental electron-transfer rate constant k_{EX} and the counterion diffusivity D_{ClO4} is expected if the right-hand term in eq 9 is dominant. That is, a solvent-dynamics-like behavior could result from control of the barrier-crossing frequency of the primary electron transfer (the first step in eq 9) by the subsequent relaxation of counterions. The rate of that relaxation would vary with counterion diffusivity. Figure 8 presented above shows that an excellent correlation between k_{EX} and D_{ClO4} indeed exists. Furthermore, Table 1 shows that, except for the unplasticized melt (zero pressure), the values of D_E and D_{ClO4} are very similar and that the values of $E_{A,ET}$ and $E_{A,ION}$ are more similar to one another than are $E_{A,ET}$ and $E_{A,PHYS}$.

It is instructive to examine whether reasonable values of the product $K_{EQ}k_2$ result from assuming that $K_{EQ}k_2 = k_{EX}$ (Table 1) and $D = D_{ClO4}$ (Table 1). If K_{EQ} is presumed to be relatively unselective (i.e., $K_{EQ} = 1$), values of a result ranging from 5 to 8 Å. If $K_{EQ} = 10^{-1}$, a values range from 2 to 3 Å. These values are a fraction of the Co complex spacing in the melt material.

(29) Newton, M. D.; Sutin, N. *Annu. Rev. Phys. Chem.* **1984**, *35*, 437.
(30) Williams, M. E.; Crooker, J. C.; Pyati, R.; Lyons, L. J.; Murray, R. W. *J. Am. Chem. Soc.* **1997**, *119*, 10249.
(31) (a) Our previous work[31b] shows that the D versus $1/\eta$ slopes vary with the chain length of poly(ethylene glycol) (PEG), but the inverse proportionality, given by the Stokes−Einstein equation, between viscosity and diffusion coefficient is maintained for various PEG melts. (b) Haas, O.; Velazquez, C. S.; Porat, Z.; Murray, R. W. *J. Phys. Chem.* **1995**, *99*, 15279.
(32) (a) Fawcett, W. R.; Opallo, M. *J. Phys. Chem.* **1992**, *96*, 2920. (b) Fawcett, W. R.; Opallo, M. *J. Electroanal. Chem.* **1993**, *349*, 273. (c) Fawcett, W. R.; Opallo, M. *J. Electroanal. Chem.* **1992**, *331*, 815.
(33) Marcus, R. A. *J. Phys. Chem. B* **1998**, *102*, 10071.

We have not previously considered the scenario of ionic relaxation as producing a solvent-dynamics-like behavior. The preceding brief introduction suggests that ionic relaxation could provide a connection between physical diffusion and electron-transfer rates that is an alternative to the earlier polyether dipole relaxation model.

Acknowledgment. This research is supported in part by the STC Program of the National Science Foundation under Agreement No. CHE-9876674, and by the Department of Energy, Division of Basic Sciences.

Supporting Information Available: Argon pressure dependencies of D_{PHYS} and D_E (Figure S1), data on concentration correction (Table S1), and transport (Table S2) for CO_2-swollen $[Co(bpy(CO_2MePEG\text{-}350)_2)_3](ClO_4)_2$ melt (PDF). This material is available free of charge via the Internet at http://pubs.acs.org.

JA026209P